# Supplementary Information

## Rif1 provides a new DNA binding interface for the Bloom syndrome complex to maintain normal replication

Dongyi Xu[1], Parameswary Muniandy[2], Elisabetta Leo[3], Jinhu Yin[1%], Saravanabhavan Thangavel[4], Xi Shen[5], Miki Ii[6#], Keli Agama[3], Rong Guo[1], David Fox 3rd[1], Amom Ruhikanta Meetei[1§], Lauren Wilson[1], Huy Nguyen[7], Nan-ping Weng[7], Steven J. Brill[6], Lei Li[5], Alessandro Vindigni[4], Yves Pommier[3], Michael Seidman[2], and Weidong Wang[1*].

# Supplementary Materials and Methods

### CHIP and eCHIP assays

These assays were performed as described previously (Shen et al., 2009; Thangavel et al., 2010).

### Chromosome aberration analysis

Cells were incubated with or without FUdR (4 μg/ml) for 8 hours, and colcemid (0.1 μg/ml) was added for the last 3 hours before harvest. Harvested cells were treated with 75 mM KCl for 20 min at room temperature and fixed with methanol-acetic acid (3:1) for 30 min. The cell suspension was dropped onto wet glass slides and air dried. The slides were stained with 3% Giemsa solution, pH 6.8 for 10 min before microscopy.

### Measure of spontaneous stalling rate of replication forks

Sequential labeling with 100 μM iododeoxyuridine (IdU) (Sigma Chemical Col, St. Louis, MO) and 100 μM chlorodeoxyuridine (CldU) (ICN, Irvine, CA) were done as described (Conti et al., 2007; Seiler et al., 2007) for 10 minutes each. Cells were harvested, washed and re-suspended in phosphate buffered saline (PBS) and 1% low-melting-point agarose to a final cell concentration of $10^5$ cells/100 μL. The suspension was aliquoted in pulsed-field gel electrophoresis molds and kept at +4$^o$C for 30 min. To prepare a protein-free solution of high molecular-weight genomic DNA, the agarose plugs were immersed in a suitable volume of 0.5 M EDTA pH 8 (250 μL per plug) and treated overnight with 1% N-lauryl sarcosyl and 1 mg/mL proteinase K (Sigma) at 50$^o$C. Complete removal of digested proteins and other degradation products was done by several gentle washings in Tris-EDTA [10mM Tris, 1mM EDTA pH8]. Protein-free DNA plugs were then stored in 0.5M EDTA (pH 8) at 4$^o$C or immediately used for combing.

Prior to combing, an agarose plug was melted at 70$^o$C for 20 min with 1.8 mL of 100 mM MES [2-(N-morpholino)ethanesulphonic acid] (pH 6.5) (Sigma, M-8250). The solution was kept at 42$^o$C for 15 min and treated overnight with 2 μL β-agarase

(New England Biolabs, Ipswich, MA). The solution was transferred to a Teflon reservoir. A sylanized coverslip surface (Microsurfaces Inc. Minneapolis, MN) was immerged in the solution to allow DNA molecules to anchor to the coverslip surface. After 5-10 min, the coverslip slide was lifted from the solution at constant velocity (0.32 mm/sec).

Coverslips with combed DNA were allowed to dry for 1.5 h at 60$^{o}$C; after which, they were incubated in 1 M NaOH for 10 min with gentle shaking to denature the DNA. After several quick washes in PBS, coverslips were incubated with primary antibodies and incubated at 22$^{o}$C in a humid chamber for one hour. Antibodies were diluted in 1% blocking solution (Roche, Indianapolis, IN) as follows: 40% for mouse anti-BrdU (BD PharMingen, San Jose, CA) and 20% for rat anti-CldU (Accurate Chemical & Scientific Corp., Wesbury, NY). After three 5 min washes in PBS, coverslips were incubated for 20 min at 37$^{o}$C with secondary antibodies: 4% donkey anti-mouse-488 (Molecular Probes, Eugene, OR) and 4% donkey anti–rat-594 (Molecular Probes). Following three washes in PBS, coverslips were mounted in Vectashield (Vector Laboratories, Burlingame, CA).

The slides were scanned with an inverted fluorescence microscope using a 40X objective. Images were recorded by IPLab software (BD Biosciences Bioimaging, Rockville, MD) and fluorescent signals were measured using ImageJ (National Cancer Institute) and analyzed in Excel. Statistical analyses were performed with Prism 5 software (GraphPad Software, Inc.).

**Measure of recovery efficiency of stalled replication forks**

To examine recovery efficiency of stalled replication forks, a method described by (Edmunds et al., 2008) was used with modifications. Cells were first labeled by IdU (20 μM) for 20 min. CldU (200 μM) and aphidicolin (100 ng/ml) then were added. After 20 min incubation, cells were harvested and resuspended in PBS to a concentration of $2.5\times10^{5}$ cells/ml. Then the cells were diluted 1:4 with unlabeled cells at the same concentration and 2.5 μl of cells was mixed with 7.5 μl lysis buffer (200 mM Tris-HCl at pH 7.5, 50 mM EDTA and 0.5% SDS) on a clean glass slide. When the edge is dried after 3-5 min, the slides were titled at 15$^{o}$ to horizontal, allowing the

DNA to flow down slowly on the slide. The slides then were are air-dried, fixed in 3:1 methanol/acetic acid and refrigerated overnight. The slides were treated with 2.5 M HCl for 1 hour, neutralized in 0.1 M $Na_3B_4O_7$, pH 8.5, and rinsed three times in PBST (PBS buffer with 0.1% Tween-20). The slides then were blocked in blocking buffer (PBST buffer containing 1% BSA) for 1 hour and incubated with primary antibodies at 4 $^oC$ overnight. The primary antibodies were diluted in blocking buffer: rat anti-BrdU (Abcam BU1/75) in 1:500 and mouse anti-BrdU (Becton Dickinson B44) in 1:20. After washes with high salt PBST (add NaCl to 500 mM) once and PBST twice, the slides were incubated at 25 $^oC$ for 1 hour with Cy3-conjugated anti-mouse IgG (Sigma, 1:3000 dilution) and Alexafluor 488-conjugated anti-rat (Molecular Probes, 1:200 dilution). After three washes with PBST, the slides were mounted in SlowFade Gold antifade reagent (Invitrogen). The slides were imaged with Zeiss Axiovert Microscope using a 100× objective. Tract lengths were measured by software AxioVision4.3.

**DT40 Immunofluorescence**

DT40 cells were treated with 2 mM HU 16 hours and centrifuged onto slides by a cytospin apparatus (Cytospin3). The cells were fixed in 2% paraformaldehyde for 10 min and permeabilized with 0.5% Triton X-100 in PBS for 5 min at room temperature. Cells were blocked in blocking buffer (5% BSA and 0.05% Tween-20 in PBS buffer) for 30 min at room temperature. The rabbit anti-Rif1 antibodies were diluted (1:3000) in blocking buffer and incubated for 1 hour at room temperature. Slides were washed 3 times with PBS and then incubated with goat anti-rabbit IgG antibodies, FITC-conjugated (VECTOR, 1:200) for 1 hour. After wash 3 times, slides were stained by DAPI and finically mounted with mounting medium (Invitrogen).

**HR-dependent DSB repair assay**

To examine HR efficiency in mammalian cells, DR-GFP reporter-contained U2OS (Xia et al., 2006) or HEK293 (Bennardo et al., 2008) cells were first transfected with siRNAs in 6-well plates at 20-25% confluence. After 48 hours, cells were transfected with I-SceI expression plasmid (pCBASce, 4 μg/well) using Lipofectamine 2000 (Invitrogen). 72 hours after the second transfection, cells were trypsinized to single

cell suspensions and analyzed by Guava Easycyte Mini System (Guava Technologies).

For HR assay in the DT40 cells, 3 million cells were transfected with 3 μg pCBASce and analyzed after 24 hours as above.

**Deletion of yeast *RIF1* and epistasis analysis.**

The yeast mutants used in this study were derived from the wild type strain W303-1a (*MAT***a** *ade2-1 ura3-1 his3-11,15 trp1-1 leu2-3,112 can1-100*) using standard techniques. The complete open reading frame of *RIF1* (YBR275C) was replaced with the *KAN* selectable marker that was constructed using PCR amplification with gene-specific primers off plasmid pUG6 (Guldener et al., 1996). Proper integrative transplacement and segregation was determined by analytical PCR. Cells were maintained on YPD plates (1% Yeast Extract, 2% Peptone, 2% Dextrose) and analyzed on YPD plates containing the indicated concentrations of HU or MMS.

**Analyses of BLM and RIF1 mRNA levels across 60 cancer cell lines**

The NCI Developmental Therapeutic Program Screen of 60 cancer cell lines (NCI60) and subsequent data analyses have been described (http://discover.nci.nih.gov/) (Reinhold et al., 2010).

## Supplementary References

Bennardo, N., Cheng, A., Huang, N. and Stark, J.M. (2008) Alternative-NHEJ is a mechanistically distinct pathway of mammalian chromosome break repair. *PLoS Genet*, **4**, e1000110.

Conti, C., Seiler, J.A. and Pommier, Y. (2007) The mammalian DNA replication elongation checkpoint: implication of Chk1 and relationship with origin firing as determined by single DNA molecule and single cell analyses. *Cell Cycle*, **6**, 2760-2767.

Edmunds, C.E., Simpson, L.J. and Sale, J.E. (2008) PCNA ubiquitination and REV1 define temporally distinct mechanisms for controlling translesion synthesis in the avian cell line DT40. *Mol Cell*, **30**, 519-529.

Guldener, U., Heck, S., Fielder, T., Beinhauer, J. and Hegemann, J.H. (1996) A new efficient gene disruption cassette for repeated use in budding yeast. *Nucleic Acids Res*, **24**, 2519-2524.

Reinhold, W.C., Mergny, J.L., Liu, H., Ryan, M., Pfister, T.D., Kinders, R., Parchment, R., Doroshow, J., Weinstein, J.N. and Pommier, Y. (2010) Exon array analyses across the NCI-60 reveal potential regulation of TOP1 by transcription pausing at guanosine quartets in the first intron. *Cancer Res*, **70**, 2191-2203.

Seiler, J.A., Conti, C., Syed, A., Aladjem, M.I. and Pommier, Y. (2007) The intra-S-phase checkpoint affects both DNA replication initiation and elongation: single-cell and -DNA fiber analyses. *Mol Cell Biol*, **27**, 5806-5818.

Shen, X., Do, H., Li, Y., Chung, W.H., Tomasz, M., de Winter, J.P., Xia, B., Elledge, S.J., Wang, W. and Li, L. (2009) Recruitment of fanconi anemia and breast cancer proteins to DNA damage sites is differentially governed by replication. *Mol Cell*, **35**, 716-723.

Thangavel, S., Mendoza-Maldonado, R., Tissino, E., Sidorova, J.M., Yin, J., Wang, W., Monnat, R.J., Jr., Falaschi, A. and Vindigni, A. (2010) The human RECQ1 and RECQ4 helicases play distinct roles in DNA replication initiation. *Mol Cell Biol*.

Xia, B., Sheng, Q., Nakanishi, K., Ohashi, A., Wu, J., Christ, N., Liu, X., Jasin, M., Couch, F.J. and Livingston, D.M. (2006) Control of BRCA2 cellular and clinical functions by a nuclear partner, PALB2. *Mol Cell*, **22**, 719-729.

Correlation in expression of BLM and RIF1 mRNA across 60 cancer cell lines from the NCI Developmental Therapeutic Program Screen (NCI60).

A

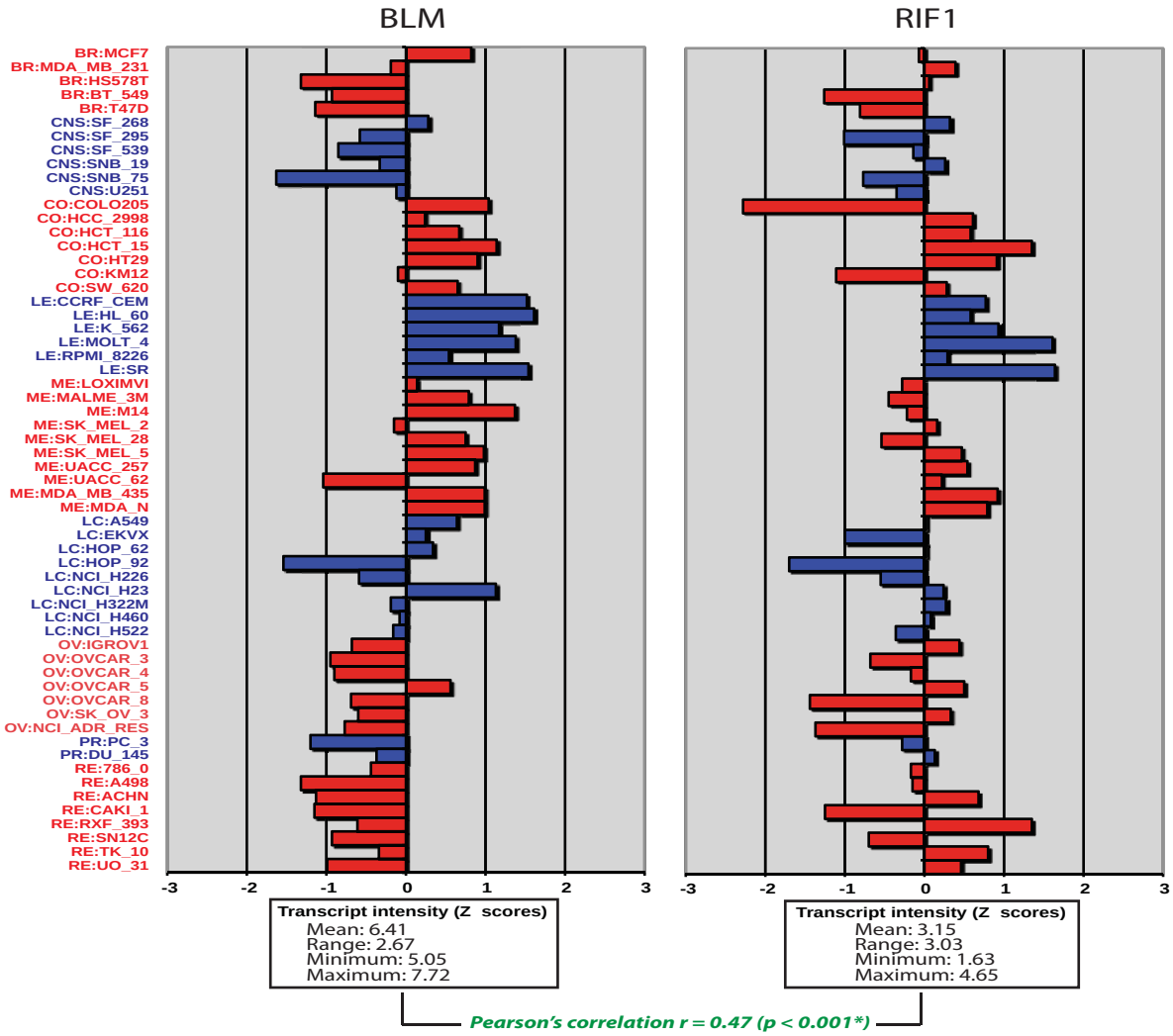


B

| | BLM | RIF1 | TOP3A | RMI1 | RMI2 (C16orf75) |
|---|---|---|---|---|---|
| BLM | **1.000** | | | | |
| RIF1 | **0.462** | **1.000** | | | |
| TOP3A | 0.215 | 0.143 | **1.000** | | |
| RMI1 | 0.402 | 0.205 | 0.218 | **1.000** | |
| RMI2 | **0.444** | 0.074 | 0.048 | 0.328 | **1.000** |

**p < 0.001**
p < 0.01
p < 0.10

Legend: (A) Graphs showing correlation between BLM and Rif1 mRNA expression in 60 cancer cell lines by microarray screening of National Cancer Institute (NCI60; http://discover.nci.nih.gov/). Gene expression was mean-centered for the 60 cell lines and deviation from the mean value for each cell line is represented as Log2 value above (positive values) or under (negative values) the mean. Red bars correspond to the breast (BR), colon (CO), melanoma (ME), ovarian (OV) and renal (RE) cell lines. Blue bars correspond to the central nervous system (CNS), leukemia (LE), lung cancer (LC) and prostate (PR) cell lines (from top to bottom)(Reinhold et al. 2010). (B) The correlations of gene expressions among BLM, Rif1, Top3A , RMI1 and RMI2. The p-values are listed on the right.

# Rif1 self-associates through its C-terminal domain

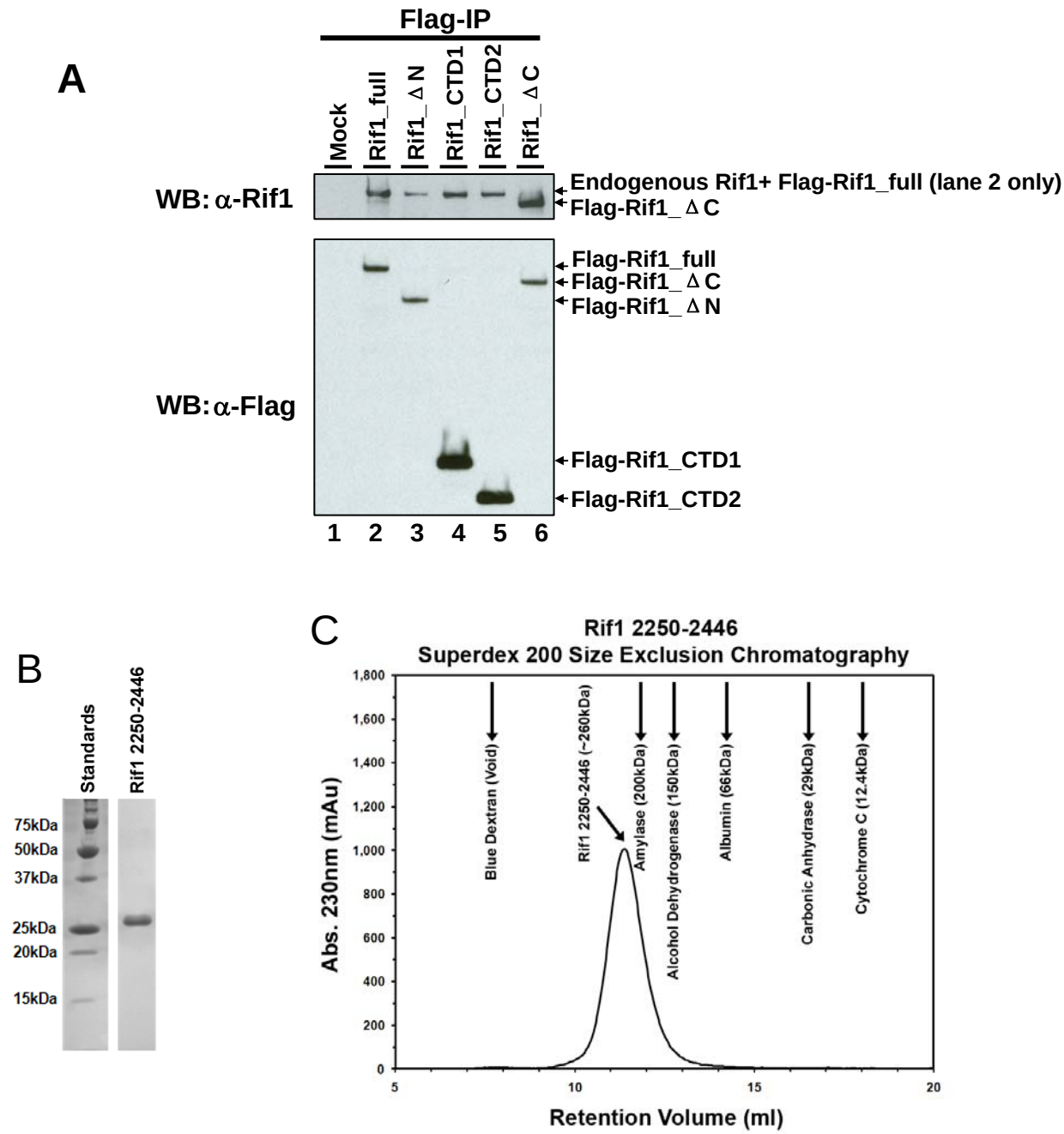


**Legend.** (**A**) IP-Western shows that Flag-tagged Rif1 deletion mutants containing intact C-terminal domain (lanes 2-5) can co-immunoprecipitate (co-IP) with endogenous Rif1 in HEK293 cells, whereas the mutant lacking the C-terminal domain (lane 6) cannot. The Rif1 constructs were described in Figure 5D. The bottom panel was also shown in Figure 5E and was included here for comparison. (**B**) SDS-PAGE of a recombinant Rif1 protein containing the C-terminal subdomains II and III (aa. 2250-2446). The protein was expressed as an 6XHis fusion protein in *E.Coli* and purified by Ni-affinity chromatography. (**C**) Gel-filtration analysis of the recombinant Rif1 protein 2250-2446 shows that it elutes with a molecular weight of about 260 kDa, which is about 10-fold bigger than its calculated weight (22 KDa), suggesting that it self-associates by oligomerization.

# A significant fraction of Rif1 in HeLa nuclear extract does not associate with BLM

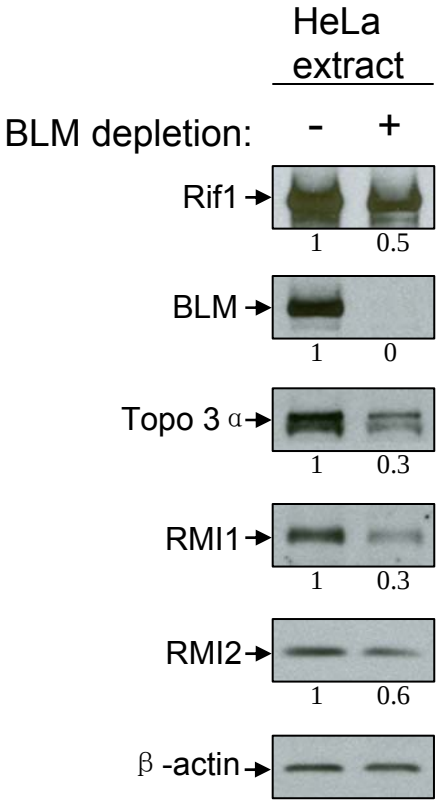


Legend: Western blotting shows that about 50% of Rif1 was co-depleted with BLM by immunoprecipitation with a BLM antibody from HeLa nuclear extract. Thus, a significant fraction of Rif1 (about 50%) does not associate with BLM. The data are consistent with the findings of gel-filtration chromatography (Figure 1D) that a subset of Rif1 can form a complex independent of BLM. The relative levels of indicated proteins to β-actin on images were calculated and shown below the blots. The protein level without depletion was set as “1”.

# The level of Rif1 protein is reduced in HEK 293 cells depleted of various BLM complex components

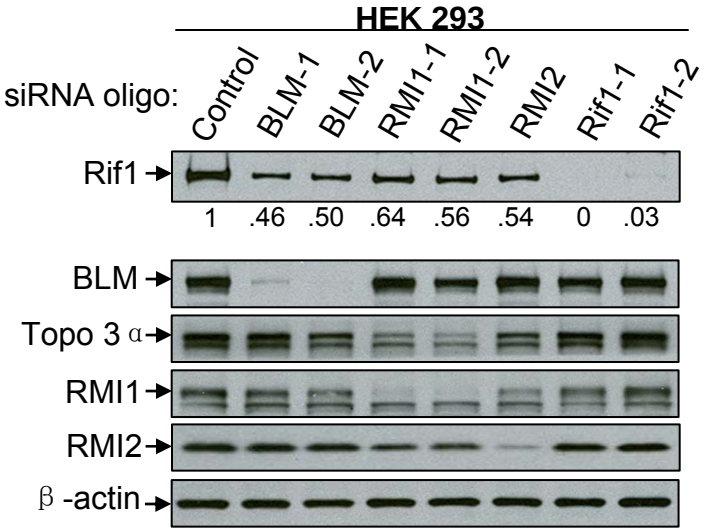


Legend. Immunoblotting shows that the Rif1 protein level is reduced in HEK 293 cells depleted of BLM, RMI1 or RMI2 by siRNA. The relative levels of Rif1 were quantified and shown between the image. The level of Rif1 in cells treated with control siRNA was set as “1”. Immunoblotting of β-actin was used as a loading control.

# Rif1 and the BLM complex are recruited together to a replication origin in cells under HU-induced replication stress

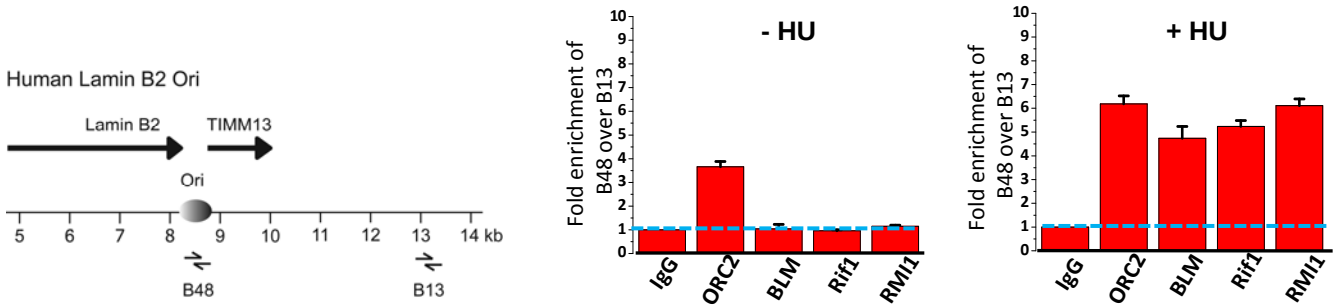


Legend. CHIP data showing that Rif1 is recruited to HU-stalled forks at a defined replication origin in Lamin B2 locus. *Left*, the genomic locus containing the lamin B2 replication origin together with the location of primers (converging arrow pairs) used for quantitative real-time PCR analysis. *Middle* and *Right*, histograms show the enrichment of target proteins at the lamin B2 origin relative to the non-origin control sequence. The antibodies used in ChIP are indicated at the bottom. The experiments were performed using T98G cells untreated or treated with 2 mM HU for 20 hours. Fold enrichments of the origin sequences (amplified by B48 primers) were determined versus non-origin control sequences (amplified by B13 primers), and the dashed lines indicate the threshold enrichment level obtained by using a negative control antibody (normal rabbit IgG). Results are reported as means ± SEM (standard error of the mean, indicated by error bars) of at least three independent experiments.

# Rif1 recruitment to an ICL is stimulated by DNA replication

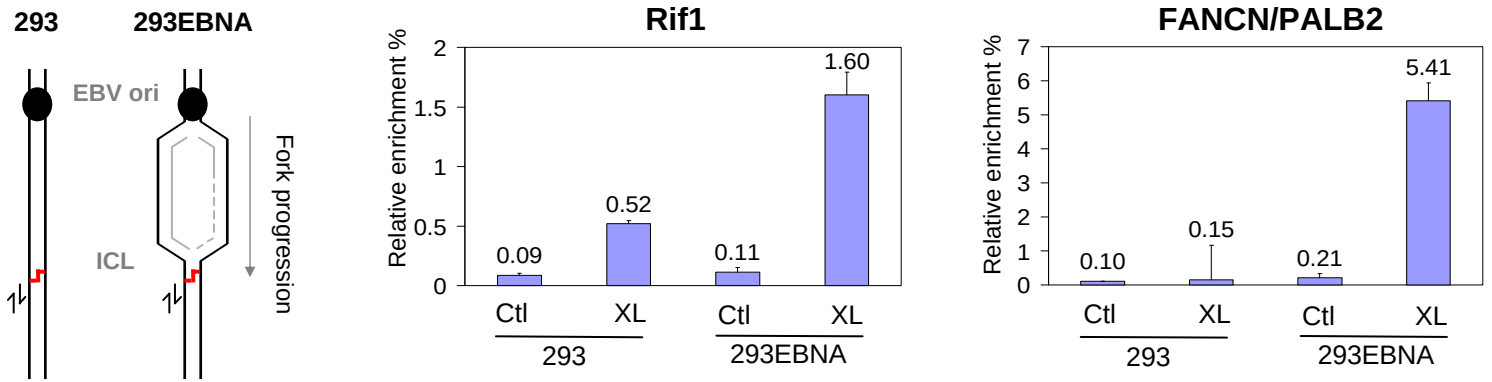


Legend. eCHIP data show that Rif1 is recruited to replication forks blocked by a defined ICL.

*Left*, schematic representation of the plasmid substrate under non-replicative and replicative states in HEK293 and HEK293-EBNA cells, respectively. EBV ori denotes EBNA supported replication origin. The position of the ICL is shown in red line. The converging arrow pairs indicate the primers for PCR amplification. *Middle* and *Right*, graphic representation of eCHIP-qPCR data for Rif1 and FANCN/PALB2, respectively. Ctl, unmodified control plasmid. XL, crosslinked plasmid. Percentages of relative enrichment were arrived by normalizing comparative concentration of each sample with that of its input.

This assay allows direct detection of proteins at a site-specific psoralen ICL on an episomal plasmid transfected into cells. The plasmid contains the replication origin of Epstein-bar virus (EBV), which supports a virtual unidirectional replication in EBNA-293 cells (which express Epstein-bar nuclear antigen 1 (EBNA1)) (left panel). A site-specific psoralen ICL is introduced into this plasmid 488 bp downstream of the replication origin prior to transfection to block the progression of replication forks. Proteins accumulated at the fork can be detected by CHIP-qPCR using a primer set that amplifies a DNA fragment near the ICL. The ratio between CHIP-qPCR signals in the presence and absence of the ICL reflects the enrichment of a target protein. In parental 293 cells that do not support replication of the plasmid, Rif1 was enriched about 5-fold at the ICL (middle panel). This is in contrast to FANCN/PALB2, which shows no significant enrichment (right panel). The data suggest that the recruitment of Rif1 to ICLs may occur without replication. In EBNA-293 cells that support vector replication, Rif1 was enriched about 15-fold at the ICL, about 3-times higher than in regular 293 cells. The data are consistent with the notion that Rif1 recruitment is enhanced by the presence of stalled replication forks at ICLs.

# The Rif1 protein level is normal in *blm*-knockout chicken DT40 cells

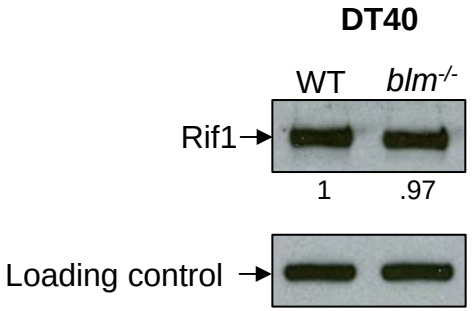


Legend. Immunoblotting shows that the Rif1 protein level in *blm*-knockout chicken DT40 cells is comparable to that of wildtype (WT) cells. The quantification of the immunoblotting signal was shown below the image. The Rif1 level in willdtype cells was set as “1”.

# Biallelic inactivation of *Rif1* gene in chicken DT40 cells

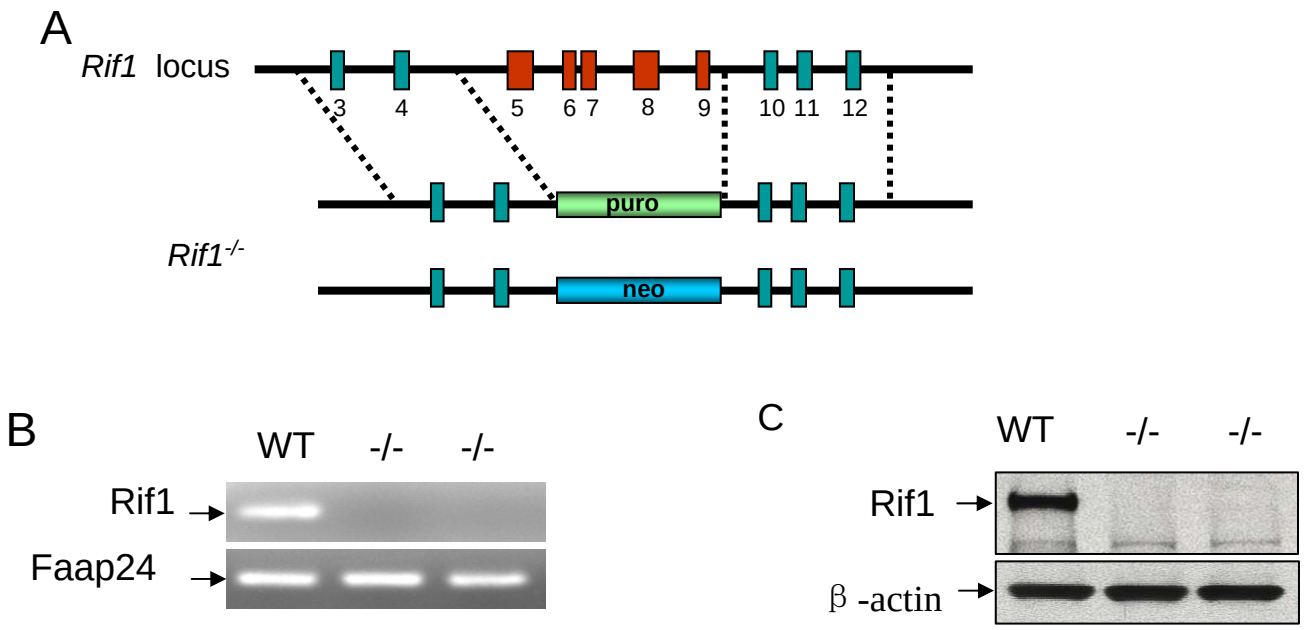


Legend. (**A**) Schematic representation of the chicken Rif1 genome locus and the targeting vectors. The region containing exon 5-9 (marked by red) of Rif1 gene is replaced by puromycin or neomycin resistant gene in the targeting vectors. The two regions between two pairs of dotted lines were used as homologous arms of the targeting constructs. (**B** and **C**) RT-PCR (**B**) and immunoblotting (**C**) show that Rif1 mRNA and protein are undetectable in two different clones of *Rif1**-/-*** DT40 cells. FAAP24 and actin were included as controls.

# Rif1 plays a role in cell proliferation in the absence of BLM.

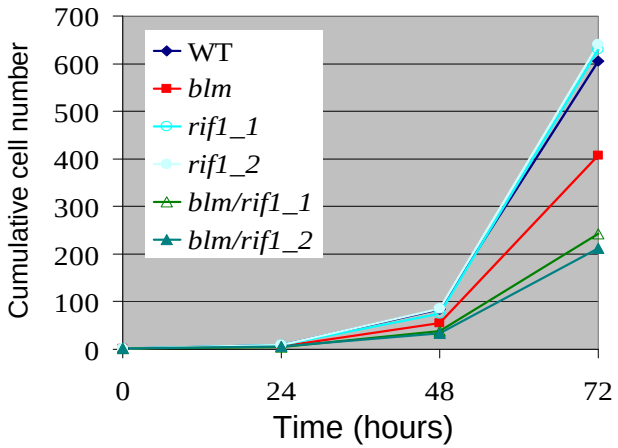


Legend. A graph showing growth curves of the cells with various genotypes. Cells were counted by flow cytometry, and at least three independent experiments were performed.

# Stalled replication forks accumulate in *rif1*$^{-/-}$ *null* DT40 cells.

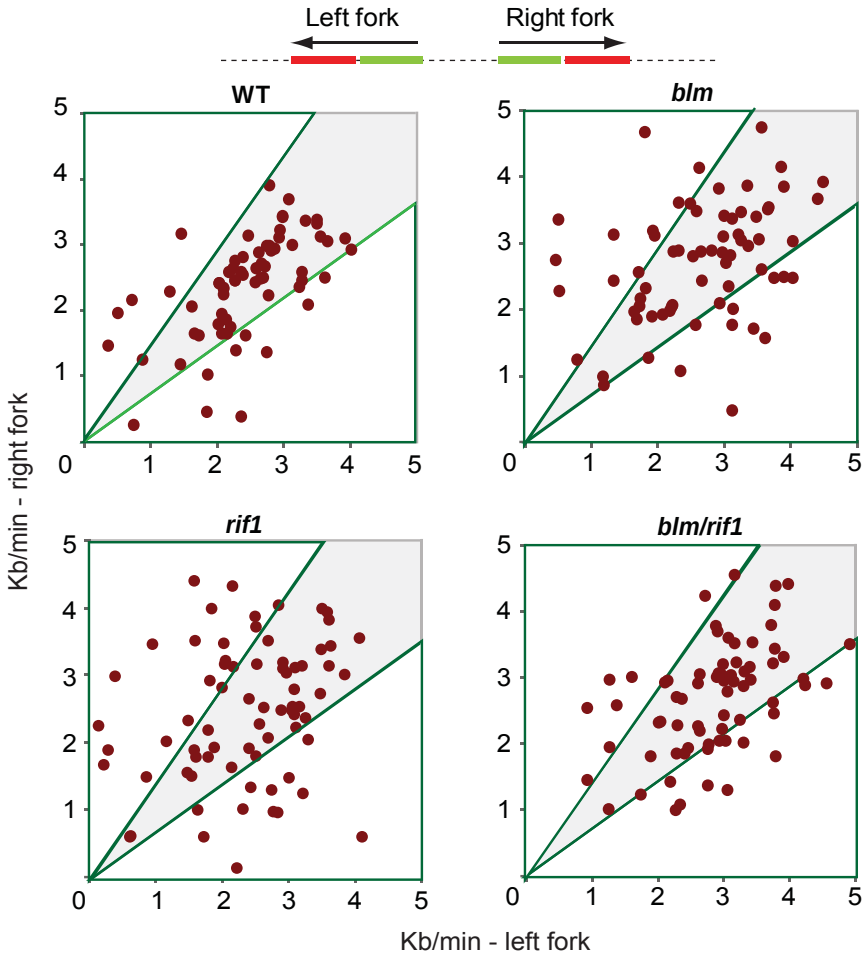


Top: schematic representation of a replicon in a DNA fiber. The bi-directional signal of the outgoing forks is monitored by two sequential equal pulses, the first the first with IdU (green) and the second with CldU (red) to allow identification of fork direction. Bottom: signals are measured and fork velocity values of left and right forks are calculated in kb/min (1 μm=2kb) considering that each pulse was 10 minutes. In the scatter diagram, each dot corresponds to the ratio between the right and the left fork velocities of a pair of outgoing forks belonging to the same replication bubble. If replicons are symmetrical, as expected in normal healthy cell lines, the left and right forks progress with similar speed, and the ratio between the (left and right) fork velocities is approximately 1. However, if one of the two forks replicates with a different speed, the ratio diverges. Those replicons for which the ratio of fork velocities deviate more than 33% from the expected theoretical value (of 1) are considered asymmetrical. This limit is marked with two green lines in each scatter diagram. The shaded areas in the plots between the green lines include all points that represent symmetrical replicons. On the contrary, the signals counted outside the two green bars (that represent the ±33% deviation from the expected theoretical value of 1) are considered asymmetrical. In the wild type cells (WT) most of the replicons are symmetrical, whereas many asymmetrical signals are present in the case of *rif* $^{-/-}$ cells.

# Rif1 has a conserved HEAT-repeat and a C-terminal domain

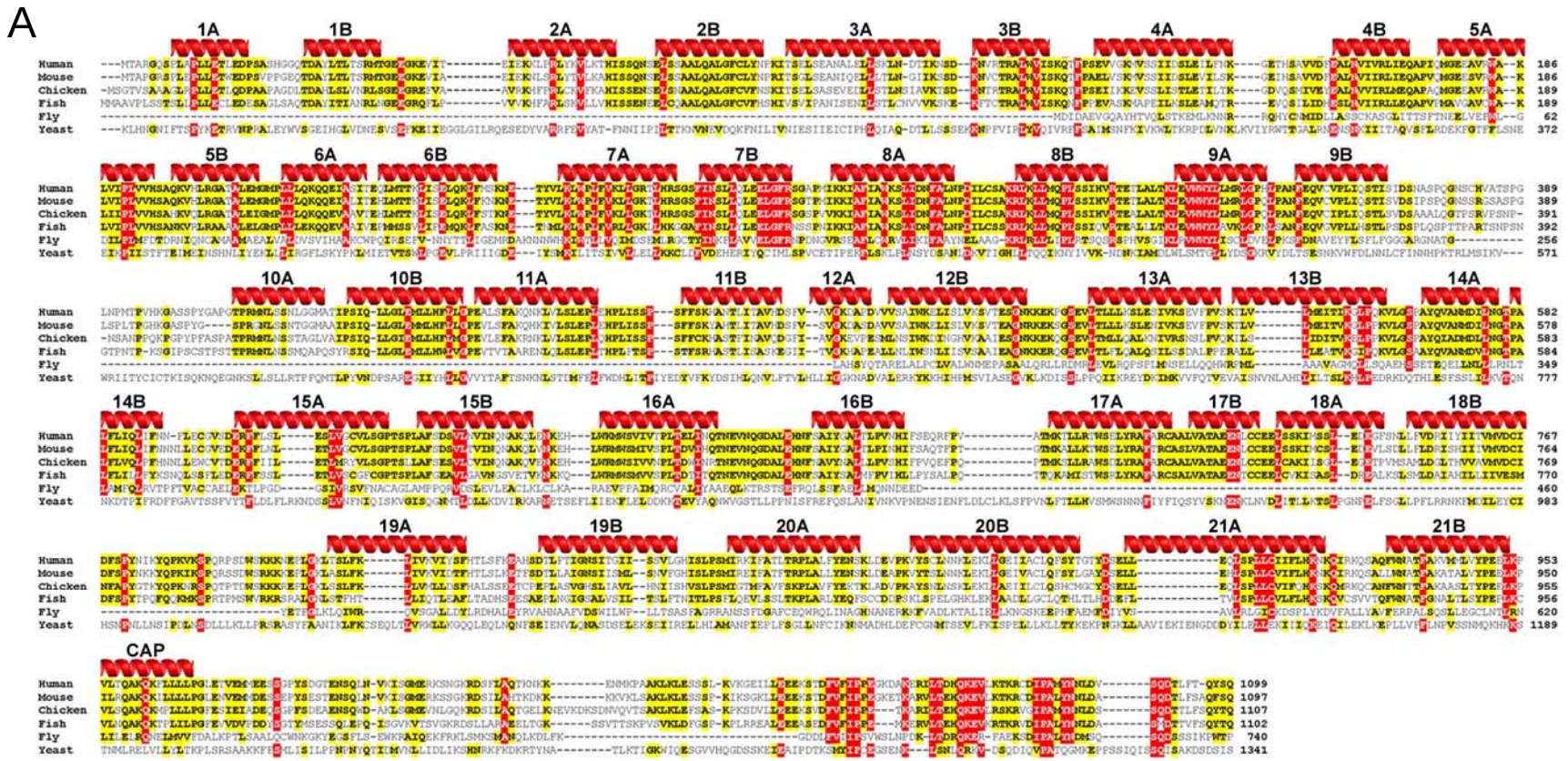


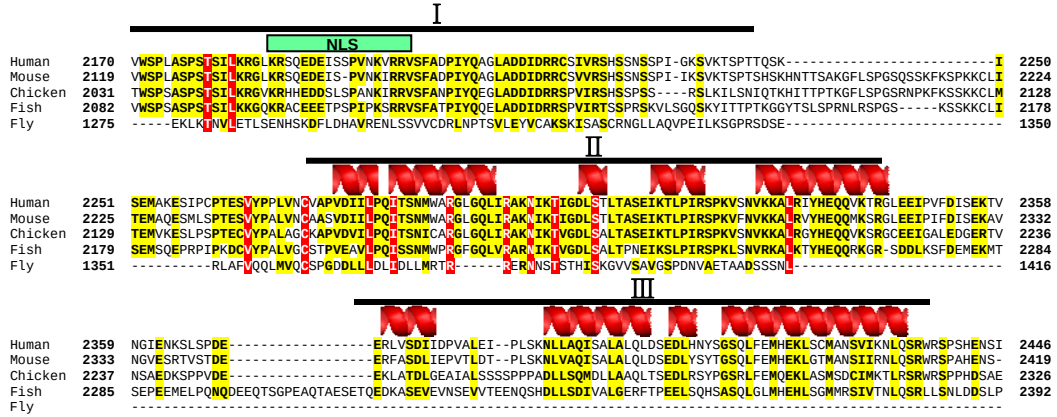


Sequence alignment of the (A) N-terminal and (B) C-terminal folded regions across species. Amino acids that are conserved in 5 or 6 species are highlighted in red, and those that are conserved in at least 4 of 6 species are highlighted in yellow. Secondary structural elements and HEAT-like repeats are indicated above the sequences (A). The protein sequences shown in (A) and (B) are indicated as figure 5A.

# The Rif1 C-terminal Domain has strong binding activity for fork and Holliday Junction DNA and low affinity for ssDNA

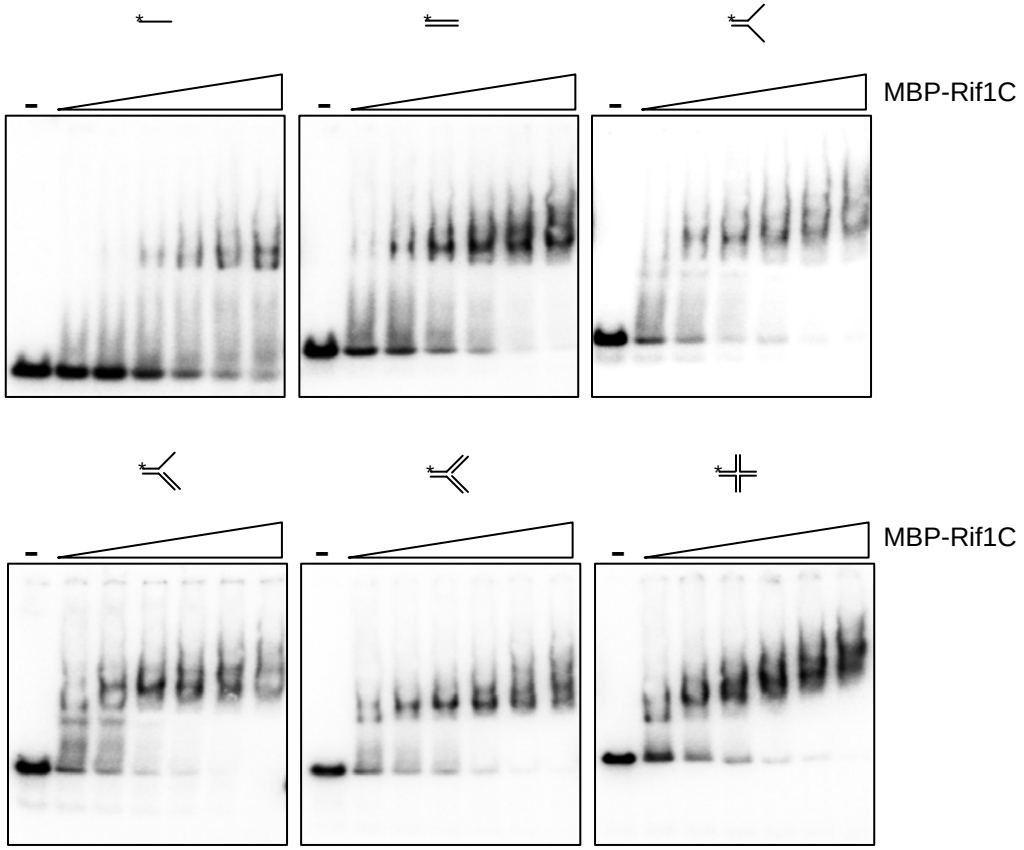


Legend. Gel-shift DNA-binding assays to show that a fusion protein of MBP and the Rif1 C-terminal domain (MBP-Rif1C) has stronger binding activity to Holliday Junction and fork substrates, and weaker affinity for ssDNA. The various synthetic DNA substrates are illustrated on the top. The $^{32}$P-labeled probe is denoted with an asterisk. The reaction mixtures contain the purified MBP-Rif1C protein of increasing concentrations (0, 50, 100, 200, 400, 800 and 1600 nM) and 1 nM of the indicated $^{32}$P-labeled substrates. The protein-DNA complexes were analyzed by 3-15% polyacrylamide gels.

# The DNA binding activity of the Rif1-αCTD domain is reduced in point Mutant A and eliminated in the double-mutant AC

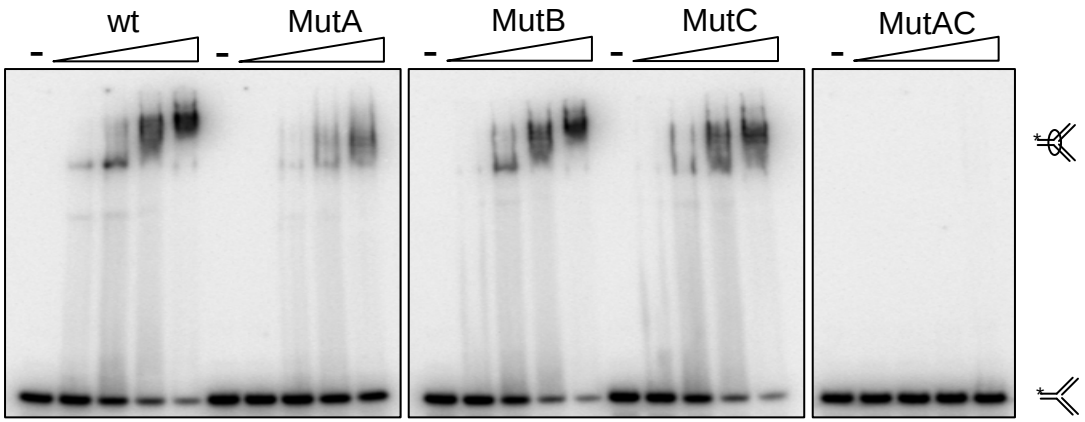


Legend. Audioradiographs of the gel-shift assay showing the DNA binding activity of wildtype (WT) or mutants of the Rif1 C-terminal domain fusion proteins (MBP-Rif1C). A graph showing quantification of these images was shown in Figure 7B. The various recombinant proteins were shown in Figure 7A. Notably, the DNA binding activity is reduced in mutant A, and completely inactivated in the double-mutant AC, which is consistent with the findings from the Southwestern DNA binding assay (Figure 7A). Reactions contained 1 nM indicated 32P-labeled fork and 0, 25, 50, 100 and 200 nM purified proteins as indicated.

# The uncropped original data showing that the hRif1-MutAC mutant co-immunoprecipitates with BLM complex

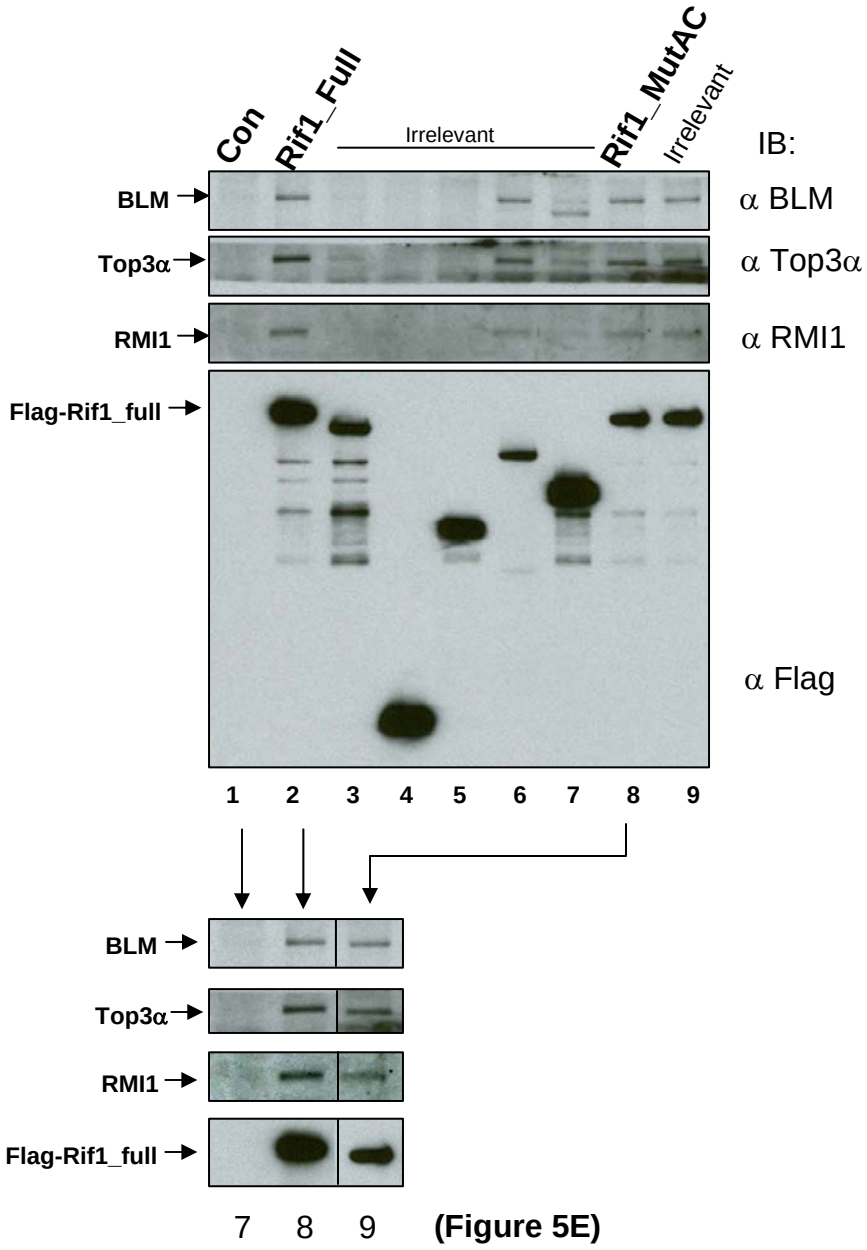


Legend. **Top:** the uncropped original immunoblotting images show that the Rif1-AC point mutant co-immunoprecipitates with BLM complex. Antibodies used for immunoblotting (IB) are shown on the right. **Bottom:** the images are spliced and assembled together using lanes 1, 2, and 8 from the top. The combined images are shown in Figure 5E, lanes 7-9. The irrelevant lanes are spliced out.

# The yeast homologs of Rif1 and BLM (Sgs1) are not epistatic with respect to tolerating drugs that inhibit DNA replication

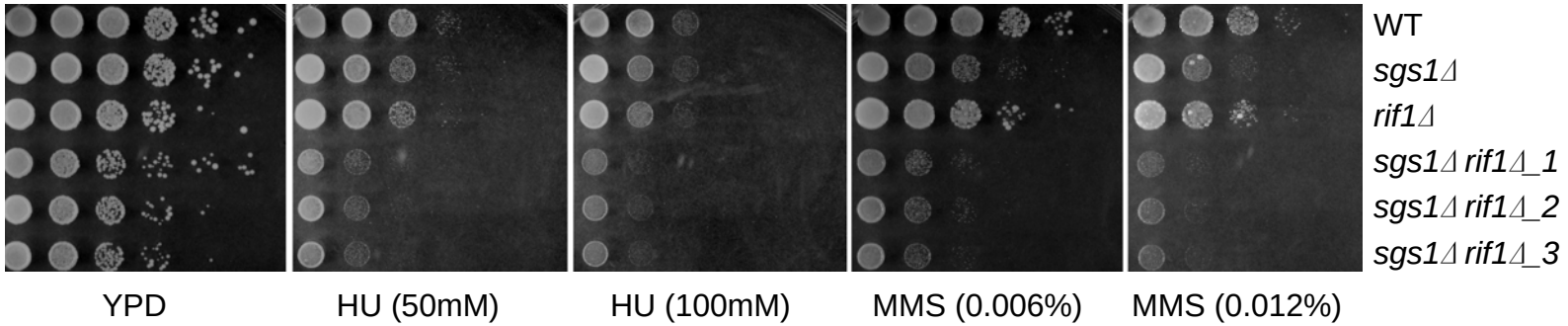


Legend. Cells of the indicated genotypes were spotted in 10-fold serial dilutions onto YPD plates with or without the indicated concentration of HU or MMS. Cells were grown at 30˚C for 2 days before being photographed.

# Rif1 is dispensable for SCE suppression and HR-dependent DSB repair and gene targeting

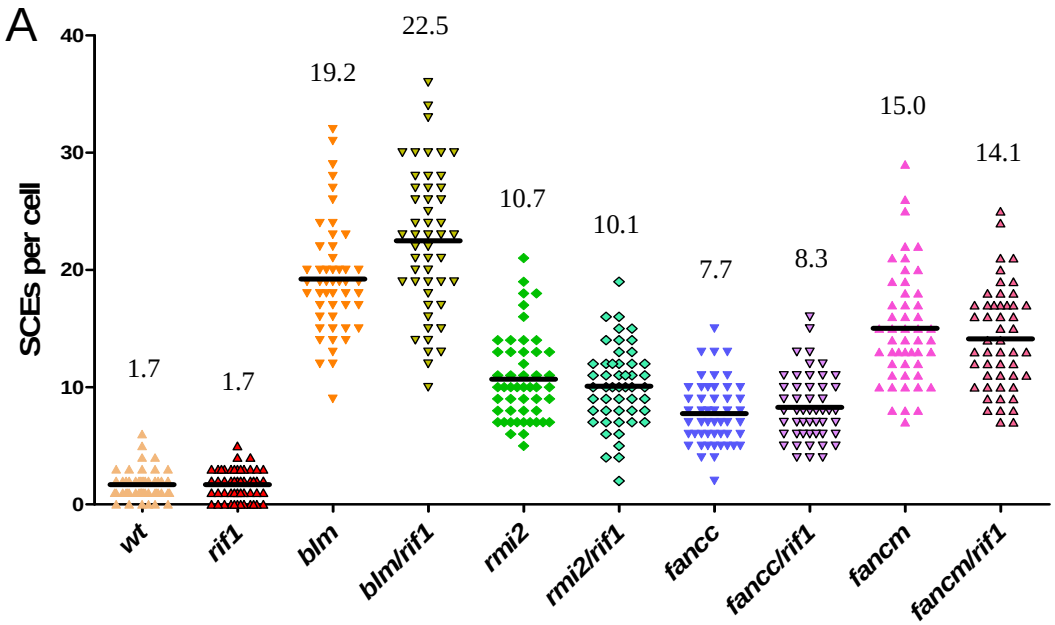


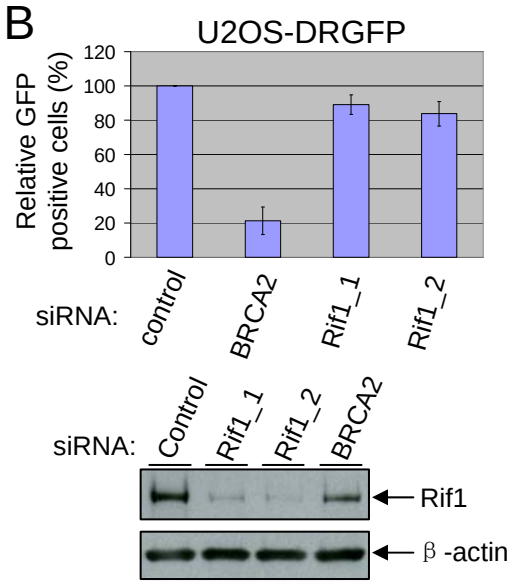


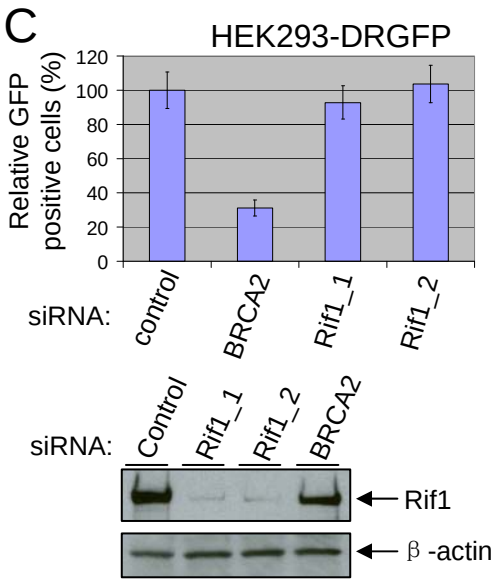


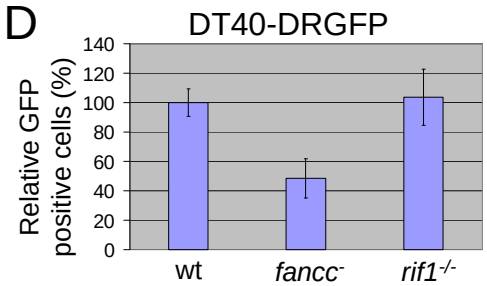


E

Gene Targeting frequency

| | wt | *rif1*$^{-/-}$ |
|---|---|---|
| OVAscneo (*puro*) | 6/55 (11%) | 10/25 (40%) |
| Δ RMI2 (*neo*) | 27/64 (42%) | 22/27 (81%) |

Legend. (A) A graph shows SCE levels of Rif1 single and various double mutant DT40 cells. (B, C, and D) Graphs showing efficiency of HR-dependent repair of double-strand breaks in Rif1-depleted U2OS cells (B) HEK293 cells (C), and *Rif1*$^{-/-}$ DT40 cells (D). The immunoblotting of Rif1 was included in (B) and (C) to show its depletion efficiency by two different siRNA oligos. (E) A table shows gene targeting efficiency in wildtype and *Rif1*$^{-/-}$ DT40 cells for two different vectors.